

Selected Paper

Preparation and Characterization of a Layered Molybdenum Trioxide with Poly(*o*-anisidine) Hybrid Thin Film and Its Aldehydic Gases Sensing Properties

Toshio Itoh,* Ichiro Matsubara, Woosuck Shin, and Noriya Izu

National Institute of Advanced Industrial Science and Technology (AIST), Shimo-Shidami, Moriyama-ku, Nagoya 463-8560

Received November 8, 2006; E-mail: itoh-toshio@aist.go.jp

Layered organic/inorganic hybrid thin film, which consist of MoO_3 with poly(*o*-anisidine) (PoANIS), were investigated by X-ray diffraction (XRD) analysis, field-emission scanning electron microscopy (FE-SEM) analysis, and gas-sensing properties analysis. The MoO_3 with PoANIS ($(PoANIS)_xMoO_3$) hybrid was prepared by an intercalation process, in which sodium ions were exchanged for PoANIS in MoO_3 thin films. The laminated structure of the $(PoANIS)_x$-MoO_3 hybrid was shown to have high periodic regularity by XRD analysis. The highly oriented $(PoANIS)_xMoO_3$ hybrid grains were observed on the substrate surface by XRD and FE-SEM analyses. The $(PoANIS)_xMoO_3$ hybrid had a large gas-sensing response to aldehydic gases, and little or no response to other volatile organic compounds. Moreover, the gas-sensing abilities of $(PoANIS)_xMoO_3$ were stronger for acetaldehyde than for formaldehyde, whereas other typical organic/MoO_3 hybrids showed an opposite response, which can be explained by solubility parameter theory.

Layered organic–inorganic hybrids have attracted much attention as novel functional materials because of their unique structure with various combinations of layered inorganic hosts and organic guests.[1,2] Layered inorganic hosts including exchangeable ions, such as clay, layered double hydroxide, and layered metal oxide semiconductor, can easily accommodate other ionic guests by ion exchange.[3–8] A notable feature of layered inorganic hosts is that their interlayer distance can expand to the size of intercalated organic molecules. Such hybrids have great potential for the development of materials with efficient properties, such as photofunctional materials,[9,10] electronic materials,[11] and mechanically modified materials, owing to hybridization.[12]

Layered orthorhombic molybdenum trioxide, MoO_3, possesses an n-type semiconducting properties. The layered structure of MoO_3 consists of double octahedra sheets that are composed of edge-sharing octahedral MoO_6 units, which have six oxygen ions and one molybdenum ion on their vertex and center, respectively. Reduced MoO_3, that is, Li_xMoO_3 or Na_xMoO_3, which is constructed with partially reduced MoO_3 with ion-exchangeable cations in the MoO_3 interlayers, is able to accommodate various organic cations. It has been reported that not only a lot of organic molecules but also several organic polymers can be intercalated into MoO_3 interlayers by several methods.[13–19]

In our previous studies, we have reported that a series of organic/MoO_3 hybrids exhibits volatile organic compound (VOCs)-gas-sensing properties.[20,21] The detection of VOCs is judged on the basis of characteristic increases or decreases in their resistive responses. These resistive responses are dominated by a change in the density of carrier electrons in the MoO_3 layers, which is caused by VOC molecules adsorbing into the MoO_3 layer frameworks or interlayer organic guests in the MoO_3 interlayers.[20,21] Other VOCs-sensing materials and systems such as metal nanoparticles,[22] porous materials,[23–25] self-assembled surfactant thin films,[26] conductive organic polymers,[27–30] carbon black with organic polymers,[31] and miniaturized gas chromatographic systems,[32] have already been reported. However, the significant and superior features of organic/MoO_3 hybrid sensors can be explained several ways. First, these sensors are capable of modifying internal organic guests to control their VOC-sensing responsiveness and selectivity. We have previously reported that organic/MoO_3 hybrids with polypyrrole and butylammonium show different response properties.[20] Second, the intercalation of several cationic organic components in MoO_3 interlayers is a simple process. In the case of thin films, the reduced MoO_3, namely, Na_xMoO_3, thin film is soaked in a solution of organic cationic components to ion-exchange sodium ions for organic cations.[33,34] Finally, the organic/MoO_3 hybrid sensors show a distinct response to aldehydic gases, whereas they have almost no response to the other VOCs, such as toluene, xylene, and methanol.[20,21] On the basis of above advantages, it is hoped that the organic/MoO_3 hybrids can be used for developing new VOC-sensing devices.

In the present study, we investigated the preparation and characterization of a poly(*o*-anisidine)-intercalated MoO_3 hybrid powder ($(PoANIS)_xMoO_3$) and its thin film, and the gas-sensing abilities of the thin film were determined. In regards to the sensing abilities, several volatile organic compounds (VOCs) were investigated, and the $(PoANIS)_xMoO_3$ hybrid thin film was found to exhibit an increase in resistive response of 4.4% to 10 ppm acetaldehyde, while it showed a 2.4% increase in the resistive response to formaldehyde and hardly any response to other VOCs.

Published on the web May 14, 2007; doi:10.1246/bcsj.80.1011

Experimental

Preparation of Na^+-Intercalated MoO_3 Powders by Reduction Process. Nitrogen gas was bubbled through 500-mL distilled water for 45 min for deaeration. Sodium hydrosulfite (4.0 g, 23 mmol; Wako Chem.) and sodium molybdate dihydrate (120 g, 0.50 mol; Kanto Chem.) powders were added into the distilled water, and the solution was stirred in bubbling nitrogen until the powders dissolved. The MoO_3 powder (10 g, 69 mmol; Kanto Chem.) was added to the solution over 3 min to reduce the MoO_3 layers and to insert Na^+ ions into the interlayers.[35] The Na^+-intercalated MoO_3, $[Na(H_2O)_2]_xMoO_3$, was washed with distilled water and then dried at 90 °C for 1 day to obtain 4.5 g of fine blue powder.

Preparation of $(PoANIS)_xMoO_3$ Hybrid Powders by Ion-Exchange Process. An aqueous suspension (25 mL) of *o*-anisidine (3.0 g, 25 mmol) was mixed with aqueous HCl (2.3 mL, 12 mol dm^{-3}); the resulting *o*-anisidine hydrochloride solution was added to sodium peroxodisulfate (75 mg, 0.33 mmol), which is a polymerization initiator. Then, the solution was stirred magnetically while bubbling with nitrogen for 30 min. The color of the solutions became reddish brown due to the polymerization of *o*-anisidine. After being stirred, the poly(*o*-anisidine) suspension was filtrated. $[Na(H_2O)_2]_xMoO_3$ powder (0.10 g) was added into the filtrate and stirred for 10 min to ion-exchange soluble poly(*o*-anisidine) with sodium ions. The resulting hybrid powder was collected by filtration, washed with ethanol and water, and then dried at 90 °C for 1 day to obtain 99 mg of fine blue powder.

Preparation of Buffer Layer on SiO_2/Si Substrate. A $LaAlO_3$ (LAO) buffer layer was prepared on a silicon wafer with a thermally oxidized SiO_2 insulating layer, abbreviated as SiO_2/Si, to adhere the MoO_3 films to the surface of the wafer effectively. The LAO-coated silicon substrate was prepared by using a solution method. The SiO_2/Si was cut into 2×2 cm^2 sections. An excess amount of LAO precursor coat solution, which was a mixture of a stoichiometric amount of 0.1 mol dm^{-3} $LaO_{1.5}$ precursor in xylene solution (Kojundo Chem.) and 3% Al_2O_3 precursor in acetic ester solution (Kojundo Chem.), was deposited on the SiO_2/Si substrate. The substrate was spin-coated at 500 rpm for 10 s to spread the solution for full substrate coverage; it was then quickly accelerated to 3000 rpm and allowed to continue spinning for 30 s. After being dried at 90 °C for 30 min, the substrate was annealed at 1000 °C for 30 min in air. The resulting substrate is referred to as LAO/SiO_2/Si.

Preparation of MoO_3 Thin Film by Chemical Vapor Deposition (CVD). The LAO/SiO_2/Si substrates were cut into 1×1 cm^2 sections. Before the deposition of MoO_3, a gold comb-type electrode, which had a 5×5 mm^2 areas with a 20 μm gap and a 20 μm linewidth, was formed on the buffer layers to measure the electrical resistance of MoO_3-based hybrid thin films. The MoO_3 thin films were prepared by the pyrolysis of molybdenum hexacarbonyl (Aldrich) in oxygen atmosphere by CVD.[36,37] The deposition experiments were performed under the following conditions: the total pressure was 110 Pa with an oxygen flow rate of 50 mL min^{-1}, the source temperature was 40 °C, the substrate temperature was 500 °C, and the deposition time was 15 min.

Insertion of Sodium Ions into Interlayers of MoO_3 Thin Films by Reduction Process. Nitrogen gas was bubbled through 15 mL of distilled water for 25 min for deaeration. Sodium hydrosulfite (2.3 mmol; Wako Chem.) and sodium molybdate dihydrate (25 mmol; Kanto Chem.) powders were added into the distilled water, and the solution was stirred in bubbling nitrogen until the powders were dissolved. The MoO_3 thin films were soaked in the solution for 25 s to reduce MoO_3 layers and to insert Na^+ ions in the interlayers.[35] The Na^+-intercalated MoO_3 films, $[Na(H_2O)_2]_xMoO_3$, were washed with distilled water quickly and then dried at 90 °C for 30 min.

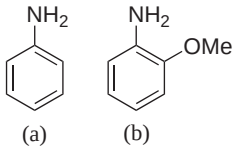

Chart 1. (a) Aniline; (b) *o*-anisidine.

Intercalation of Poly(*o*-anisidine) or Polyaniline into Interlayers of MoO_3 Thin Films by Ion-Exchange Process. An aqueous suspension (15 mL) of *o*-anisidine or aniline, as shown in Chart 1, (16.4 mmol) was mixed with aqueous HCl (1.5 mL, 12 mol dm^{-3}); the resulting *o*-anisidine or aniline hydrochloride solution was added to sodium peroxodisulfate (0.22 mmol) as a polymerization initiator. The solution was then stirred magnetically while bubbling with nitrogen for 30 min. The color of the solutions became reddish brown and dark blue due to the polymerization of *o*-anisidine and aniline, respectively. After being stirred, $[Na(H_2O)_2]_xMoO_3$ films were soaked in the suspension for 30 s to ion-exchange Na^+ with soluble poly(*o*-anisidine) or polyaniline. The resulting hybrid films were washed with distilled water quickly and then dried at 90 °C for 30 min. Poly(*o*-anisidine) and polyaniline are referred to as PoANIS and PANI, and the corresponding MoO_3 hybrids are referred to as $(PoANIS)_xMoO_3$ and $(PANI)_xMoO_3$, respectively. Scheme 1 shows the intercalation procedure for $(PoANIS)_xMoO_3$ and $(PANI)_xMoO_3$ hybrid thin films.

X-ray Diffraction Analysis of Hybrids. X-ray diffraction analysis (XRD) of MoO_3, $[Na(H_2O)_2]_xMoO_3$, $(PANI)_xMoO_3$, and $(PoANIS)_xMoO_3$ hybrids was carried out with a Rigaku RINT-2100 XRD apparatus with Cu Kα set at 1.54 Å, and operating at 40 kV and 30 mA. The XRD patterns were measured in the $2\theta/\theta$ mode within a 2θ range of 2–60° with a scan rate of 3 deg min^{-1}.

Thermogravimetry and Differential Thermal Analysis of the $(PoANIS)_xMoO_3$ Hybrid Powders. The thermogravimetry (TG) and differential thermal analyses (DTA) of the $(PoANIS)_xMoO_3$ hybrid powders was carried out with an Ulvac TGD7000RH-S TG/DTA instrument. About 12 mg of powder was placed into an alumina vessel and heated at a rate of 10 °C min^{-1} up to 600 °C in air.

Field-Emission Scanning Electron Microscopy Analysis of Hybrids. Field-emission scanning electron microscopy analysis (FE-SEM) was carried out with a JEOL JSM-6355FM microscope. All of the substrates were attached with Ag paste to the sample holder, and then dried at 90 °C for 90 min under vacuum before analysis.

Electric Properties Analysis of Hybrids. The gas-sensing properties of the $(PoANIS)_xMoO_3$ hybrid were measured in a flow apparatus, as shown in Fig. 1. Aldehydic gases, which were 181.0 ppm formaldehyde in nitrogen and 192.0 ppm acetaldehyde in nitrogen, were made by Sumitomo Seika Chemicals Co., Ltd. Chloroform, alcohols, acetone, and aromatics gases were generated by a Gastec PD-1B gas-generation apparatus. These gases were used as standard VOC gases in the sensing properties measurement. A couple of gold wires were attached to the gold comb-type electrode using silver paste. The $(PoANIS)_xMoO_3$ thin film was placed in the homeothermic chamber heated at 100 °C, and the re-

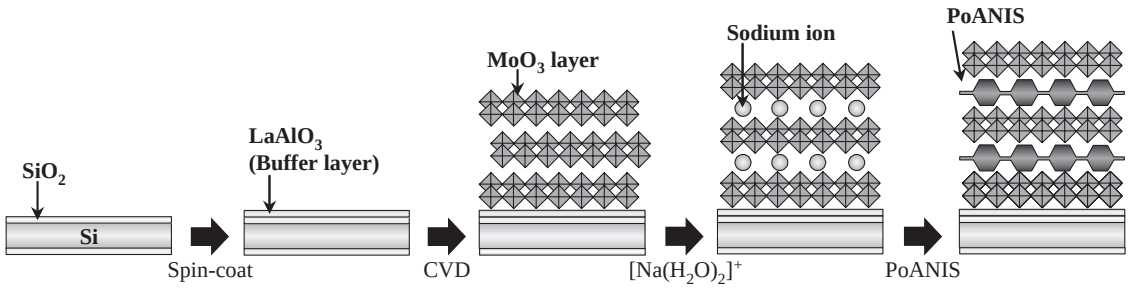

Scheme 1. Schematic depiction of preparation for $(PoANIS)_xMoO_3$ and $(PANI)_xMoO_3$ hybrid thin films.

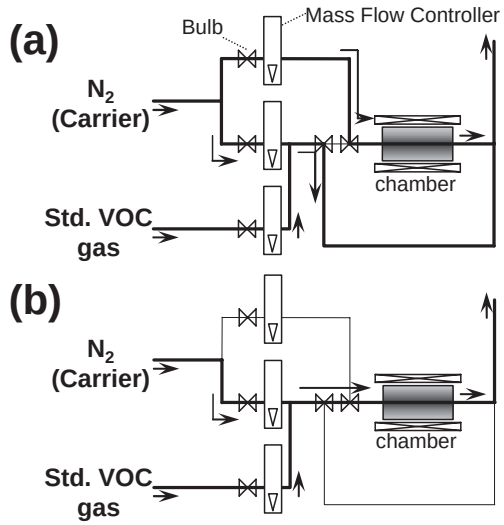

Fig. 1. Schematic diagram of a flow apparatus for the VOCs-sensing properties analysis. The $(PoANIS)_xMoO_3$ hybrid thin film was placed in the homeothermic chamber. Arrows indicate gas flow directions: (a) the pure nitrogen gas was flowed, and (b) 10 ppm VOCs with nitrogen carrier was flowed in the chamber.

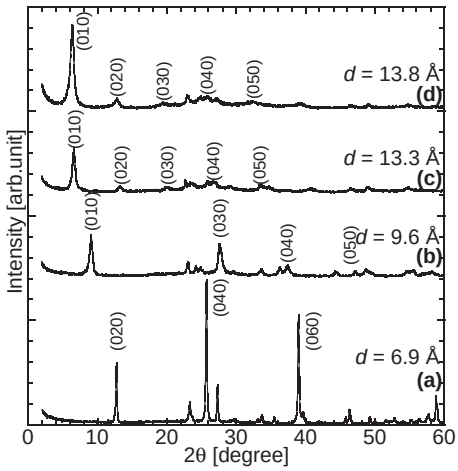

Fig. 2. XRD patterns of the (a) MoO_3, (b) $[Na(H_2O)_2]_x$-MoO_3, (c) $(PANI)_xMoO_3$, and (d) $(PoANIS)_xMoO_3$ hybrid powders measured at ca. 20 °C. The d values mean the interlayer distances of powders from (0k0) peaks.

sistance signal of the hybrid was measured directly through the gold wires. The VOC concentrations were precisely controlled by the flow system with a mass flow controller. The total flow was always 200 mL min^{-1}. After pure nitrogen gas was flowed, VOCs with a nitrogen carrier, which was a dilution of standard VOC gases with nitrogen carrier, were flowed for 10 min, and then the flow gas was again changed to pure nitrogen gas. The response was defined as Eq. 1,

$$S = \frac{R_g}{R_a} - 1, \quad (1)$$

where S, R_g, and R_a denote the response, the resistances in VOCs and pure nitrogen gas just before VOCs flowed to the chamber, respectively.

Results and Discussion

Structural Study of $(PoANIS)_xMoO_3$ Hybrid. The $(PoANIS)_xMoO_3$ hybrid powder was synthesized in order to characterize it. The series of (0k0) XRD peaks for the $(PoANIS)_xMoO_3$ hybrid powder showed characteristic high periodic regularity in its alternating laminating structure, as can be seen in Fig. 2. The (010) diffraction peak of the $[Na(H_2O)_2]_xMoO_3$ powder shifted from the MoO_3 (020) peak to a lower angle, and the series of MoO_3 (0k0) peaks disappeared, indicating the expansion of interlayer spaces by 2.7 Å due to the intercalation of sodium ions. The (0k0) peaks of $(PoANIS)_xMoO_3$ hybrid powder shifted downward from that of $[Na(H_2O)_2]_xMoO_3$ powder with an increase in the volume of the guest ions, as shown in Fig. 2. The interlayer distance of the $(PANI)_xMoO_3$ hybrids was in agreement with the molecular size of the benzene ring, indicating a perpendicular orientation of PANI chains to the MoO_3 sheets. In the case of the $(PoANIS)_xMoO_3$ hybrid, the interlayer distance was almost the same as that for the $(PANI)_xMoO_3$ hybrid, even though PoANIS has a methoxy group into ortho position. These results suggest that the benzene rings of PoANIS are tilted from the normal line against the MoO_3 layer. On the basis of structural calculations of aniline and *o*-anisidine trimers using MM2 calculations, the benzene rings of aniline queued up in parallel, while those of *o*-anisidine were alternately tilted.

Figure 3 shows the TG/DTA curve of $(PoANIS)_xMoO_3$ hybrid powder. Heat treatment up to 270 °C caused endothermic weight loss for the $(PoANIS)_xMoO_3$ hybrid, which was attributed to the release of adsorbing water and/or internal crystal water, and exothermic weight loss of 14.5% over 270 °C, which may be due to the thermal decomposition of the intercalated PoANIS. From the weight loss in the TG curve, the x value of the $(PoANIS)_xMoO_3$ hybrid was calculated to be 0.21. The elemental analysis data of dried $(PoANIS)_xMoO_3$ hybrid powder (C, 10.55; H, 1.48; N, 1.74%) was used to determine the chemical formula $(C_7H_8ON)_{0.21}MoO_3 \cdot 0.39H_2O$, indicat-

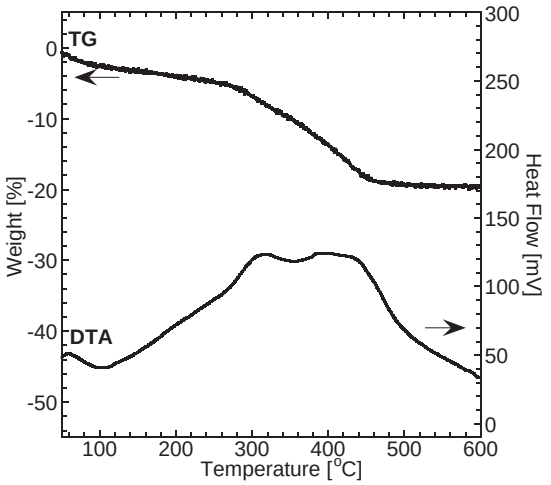

Fig. 3. TG and DTA patterns of the $(PoANIS)_xMoO_3$ hybrid in air.

ing water molecules intercalated into the MoO_3 interlayers during the reduction and ion-exchange processes.

Characterization of $(PoANIS)_xMoO_3$ Hybrid Thin Films. For the measurements of the electrical properties, the $(PoANIS)_xMoO_3$ hybrid should be processed into a thin film on a comb-type electrode. However, it is difficult to form the hybrid into as a thin film owing to the different chemical and physical properties of the organic guest and inorganic MoO_3 host. Therefore, the preparation of the $(PoANIS)_xMoO_3$ hybrid thin film was carried out in the following order: 1) deposition of MoO_3 thin films on silicon substrate with $LaAlO_3$ (LAO) buffer layer and gold comb-type electrode by a chemical vapor deposition method (CVD); 2) insertion of sodium ions into a MoO_3 interlayers by a reduction process; and 3) intercalation of organic components into MoO_3 interlayers by an ion-exchange process.

Figure 4 shows XRD patterns of the MoO_3 and MoO_3-based hybrids thin films. The series of (0*k*0) XRD peaks for the MoO_3 and MoO_3-based hybrids thin films also showed the characteristic high periodic regularity. In addition, interlayer distances of thin films were almost same value as those of powders, indicating that fine layered MoO_3 thin film can be made on $LAO/SiO_2/Si$ substrate by CVD. Trace (a) in Fig. 4 is the pattern of the MoO_3 thin film deposited on the surface of the $LAO/SiO_2/Si$ substrate. The (010) diffraction peak of $[Na(H_2O)_2]_xMoO_3$ thin film is also shown (Fig. 4b). It showed that the thin film was prevented from peeling off during an intercalation of sodium ions due to a reduction process. Traces (c) and (d) are the patterns of the $(PANI)_xMoO_3$ and $(PoANIS)_xMoO_3$ hybrids, respectively. Moreover, all of the XRD patterns in Fig. 4 showed only (0*k*0) peaks, indicating that MoO_3, $[Na(H_2O)_2]_xMoO_3$, and $(PoANIS)_xMoO_3$ hybrid films have their *b*-axis oriented highly toward the normal line against the substrate which have the LAO buffer layer. These results of XRD profiles were reproducible with independent specimens. The lattice mismatch between the in-plane average length of the *a*- and *c*-axes of MoO_3 (orthorhombic) and the *a*-axis of LAO (cubic) was 1.0%. MoO_3, $[Na(H_2O)_2]_xMoO_3$ and organic/MoO_3 hybrid grains can form *b*-axis oriented highly not on large lattice mismatch substrates, such as

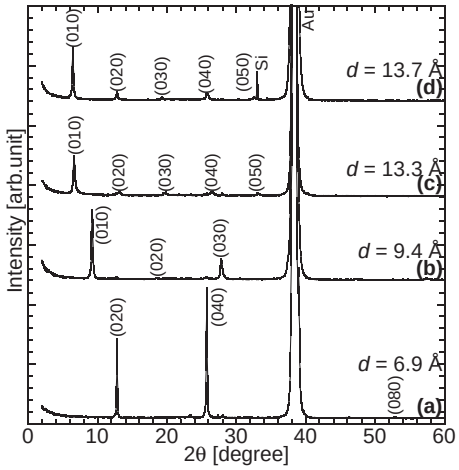

Fig. 4. X-ray diffraction patterns of the MoO_3 and MoO_3-based hybrids thin films on the $LAO/SiO_2/Si$ substrate measured at ca. 20 °C: (a) MoO_3; (b) $[Na(H_2O)_2]_xMoO_3$; (c) $(PANI)_xMoO_3$ hybrid; and (d) $(PoANIS)_xMoO_3$ hybrid. The *d* values mean the interlayer distances of thin films from (0*k*0) peaks.

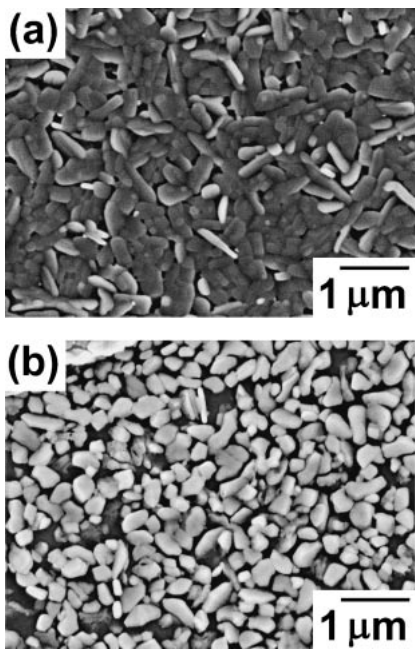

Fig. 5. The surface images of (a) MoO_3 and (b) $(PoANIS)_xMoO_3$ hybrid thin films by FE-SEM.

MgO, but on LAO single crystal substrate.[14] In addition, *b*-axis oriented MoO_3 hybrids including butylammonium ions on the LAO buffer layer has been reported.[38] The LAO buffer layer is explained to have been crystallized. Figure 5 shows the surface appearance of MoO_3 and $(PoANIS)_xMoO_3$ hybrids. The MoO_3 film consisted of oval-like thin grains, which were oriented toward the plane of the substrate surface and combined together (Fig. 5a). The hybrid grains should peel off of the substrate unless the MoO_3 grains are oriented toward the substrate, because the expanded layered MoO_3 grains interfere with each other during the intercalation of sodium ions and PoANIS into the MoO_3 interlayers. The $(PoANIS)_xMoO_3$ hy-

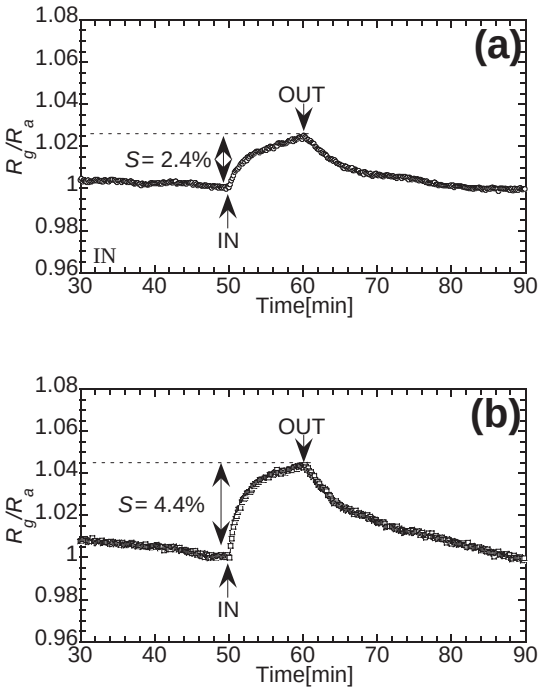

Fig. 6. Normalized resistive profiles of $(PoANIS)_xMoO_3$ hybrid. After the pure nitrogen gas was flowed, 10 ppm VOCs with nitrogen carrier were flowed for 10 min, and then the flow gas was again changed to the pure nitrogen gas. VOCs are (a) 10 ppm formaldehyde and (b) 10 ppm acetaldehyde.

brid film had grain sizes of approximately 300 nm (Fig. 5b). The electric resistance of the $(PoANIS)_xMoO_3$ hybrid film was measured on the mega ohm level to be approximately $6 \times 10^7\ \Omega$ under a nitrogen atmosphere at 100 °C, because $(PoANIS)_xMoO_3$ hybrid grains were prevented from peeling off.

Electric Properties of $(PoANIS)_xMoO_3$ Hybrid Thin Films. Figure 6 shows the increasing resistive response of the $(PoANIS)_xMoO_3$ hybrid thin film to aldehydic gases. The increase in S was 2.4% in the presence of 10 ppm formaldehyde for 10 min. An increase in S of 4.4%, when the $(PoANIS)_xMoO_3$ hybrid thin film was exposed to 10 ppm of acetaldehyde for 10 min, was also observed. The magnitudes of the responses of the $(PoANIS)_xMoO_3$ hybrid and the $(PANI)_xMoO_3$ hybrid to formaldehyde, acetaldehyde, and several other VOCs are summarized in Table 1. The $(PoANIS)_x$-MoO_3 hybrid showed an increase in resistive response to aldehydic and alcohol gases; in particular, there was a distinct response to aldehydic gases. In contrast, the $(PoANIS)_xMoO_3$ hybrid showed no response to chloroform, acetone, aromatics. These results indicate that the sensing properties of the $(PoANIS)_xMoO_3$ hybrid are affected by functional groups of the VOCs. The $(PoANIS)_xMoO_3$ hybrid thin film exhibited the same level of performance as the $(PANI)_xMoO_3$ hybrid. The organic/MoO_3 hybrids have a great potential to detect aldehydic gases.

It should be noted that the sensing properties of the $(PoANIS)_xMoO_3$ hybrid in terms of response to aldehydic gases were different from those of the $(PANI)_xMoO_3$ hybrid,

Table 1. Magnitudes of the Response (S) of the $(PoANIS)_x$-MoO_3 and the $(PANI)_xMoO_3$ Hybrids to Several VOCs and Solubility Parameters of the VOCs

VOCs	S/%		Solubility parameter /$(MPa)^{1/2}$
	$(PoANIS)_xMoO_3$ [a)]	$(PANI)_xMoO_3$ [b)]	
Formaldehyde	2.4	8.0	—
Acetaldehyde	4.4	3.8	21.1
Chloroform	<0.1	0.3	19.0
Methanol	0.5	0.2	29.7
Ethanol	0.3	0.3	26.0
Acetone	<0.1	<0.1	20.3
Benzene	<0.1	—	18.8
Toluene	<0.1	<0.1	18.2
Xylene	<0.1	<0.1	18.0

a) 10 ppm VOCs. b) 50 ppm VOCs (Ref. 38).

as shown in Table 1. Typical organic/MoO_3 hybrids, e.g., the $(PANI)_xMoO_3$ hybrid, showed the strongest response to formaldehyde, medium response to acetaldehyde, and little response to *n*-butylaldehyde and *n*-hexylaldehyde, indicating that molecular sizes of aldehydic molecules affect the sensing properties of the organic/MoO_3 hybrids. However, the $(PoANIS)_xMoO_3$ hybrid responded to acetaldehyde more strongly than to formaldehyde, as shown in Fig. 6. The normalized resistances of the $(PANI)_xMoO_3$ hybrid increased to 8.0 and 3.8% in response to 50 ppm formaldehyde and acetaldehyde, respectively,[39] while those of the $(PoANIS)_xMoO_3$ hybrid increased to 2.4 and 4.4% in response to 10 ppm formaldehyde and acetaldehyde, respectively. The signals of two sensors that respond differently to two target chemicals should be calculated to determine the exact concentrations of them. It is expected that the $(PoANIS)_xMoO_3$ hybrid can be used with typical organic/MoO_3 hybrids for the detection and determination of the exact concentration of formaldehyde and acetaldehyde.

The resistive transitional response of organic/MoO_3 hybrids was caused by VOCs that penetrate into their interlayers.[20] Therefore, the interaction of VOCs and interlayer organic components affects the VOC sensing properties. These results can be explained by the solubility parameter. The solubility of a solvent in a polymer is improved when the solubility parameter values of the polymer and the solvent are close to each other. The values of the solubility parameter for solvents are based on their heat of vaporization.[40] The values for polymers are given as Eq. 2.

$$\delta = \frac{\rho}{M} \times \sum F_i, \tag{2}$$

where δ, ρ, M, and F_i denote the solubility parameter [$(MPa)^{1/2}$], density [$g\,cm^{-3}$], molecular weight per unit, and group molar attraction constants, respectively.[41] The solubility parameters of PANI and PoANIS were calculated to be 19.1 and 20.5 $(MPa)^{1/2}$ using Small's and Hoy's F_i constants.[40–42] The solubility parameter of acetaldehyde has been reported to be 21.1 $(MPa)^{1/2}$,[40] indicating that acetaldehyde penetrates into PoANIS better than into PANI. Therefore, the large response to acetaldehyde was obtained with the $(PoANIS)_x$-MoO_3 hybrid.

Conclusion

In the present work, the sensing properties of $(PoANIS)_x$-MoO_3 hybrid thin films were investigated. The $(PoANIS)_x$-MoO_3 hybrid detected aldehydic gases, whereas it had no response toward other VOCs. The $(PoANIS)_xMoO_3$, in addition, showed a stronger response to acetaldehyde than to formaldehyde because of the high solubility of acetaldehyde into the interlayer organic components of PoANIS. The responsiveness to aldehydic gases can be controlled by the organic components.

This work was partially supported by New Energy and Industrial Technology Development Organization (NEDO). We would like to express our thanks for their kind supports.

References

1 M. Ogawa, K. Kuroda, *Chem. Rev.* **1995**, *95*, 399.
2 M. Ogawa, K. Kuroda, *Bull. Chem. Soc. Jpn.* **1997**, *70*, 2593.
3 T. Sasaki, M. Watanabe. *J. Am. Chem. Soc.* **1998**, *120*, 4682.
4 U. Costantino, N. Coletti, M. Nocchetti, G. G. Aloisi, F. Elisei, *Langmuir* **1999**, *15*, 4454.
5 P. C. LeBaron, T. J. Pinnavaia, *Chem. Mater.* **2001**, *13*, 3760.
6 R. Roto, A. Yamagishi, G. Villemure, *J. Electroanal. Chem.* **2004**, *572*, 101.
7 H. Sato, Y. Hiroe, K. Tamura, A. Yamagishi, *J. Phys. Chem. B* **2005**, *109*, 18935.
8 T. Itoh, T. Shichi, T. Yui, H. Takahashi, Y. Inui, K. Takagi, *J. Phys. Chem. B* **2005**, *109*, 3199.
9 T. Shichi, K. Takagi, *J. Photochem. Photobiol., C* **2000**, *1*, 113.
10 T. Takata, K. Shinohara, A. Tanaka, M. Hara, J. N. Kondo, K. Domen, *J. Photochem. Photobiol., A* **1997**, *106*, 45.
11 D. B. Mitzi, *Chem. Mater.* **2001**, *13*, 3283.
12 A. Usuki, Y. Kojima, M. Kawasumi, A. Okada, Y. Fukushima, T. Kurauchi, O. Kamigaito, *J. Mater. Res.* **1993**, *8*, 1179.
13 I. Matsubara, K. Hosono, N. Murayama, W. Shin, N. Izu, *Bull. Chem. Soc. Jpn.* **2004**, *77*, 1231.
14 K. Hosono, I. Matsubara, N. Murayama, W. Shin, N. Izu, *Chem. Mater.* **2005**, *17*, 349.
15 L. Han, X. Shi, W. Wu, F. L. Kirk, J. Luo, L. Wang, D. Mott, L. Cousineau, S. I. Lim, S. Lu, C. Zhong, *Sens. Actuators, B* **2005**, *106*, 431.
16 K. J. Albert, D. R. Walt, D. S. Gill, T. C. Pearce, *Anal. Chem.* **2001**, *73*, 2501.
17 M. H. Keefe, R. V. Slone, J. T. Hupp, K. F. Czaplewski, R. Q. Snurr, C. L. Stern, *Langmuir* **2000**, *16*, 3964.
18 M. P. Siegal, W. G. Yelton, D. L. Overmyer, P. P. Provencio, *Langmuir* **2004**, *20*, 1194.
19 D. L. Dermody, R. M. Crooks, T. Kim, *J. Am. Chem. Soc.* **1996**, *118*, 11912.
20 A. L. Kukla, Y. M. Shirshov, S. A. Piletsky, *Sens. Actuators, B* **1996**, *37*, 135.
21 J. Feng, A. G. MacDiarmid, *Synth. Met.* **1999**, *102*, 1304.
22 J.-S. Kim, S.-O. Sohn, J.-S. Huh, *Sens. Actuators, B* **2005**, *108*, 409.
23 A. A. Athawale, M. V. Kulkarni, *Sens. Actuators, B* **2000**, *67*, 173.
24 B. C. Sisk, N. S. Lewis, *Sens. Actuators, B* **2005**, *104*, 249.
25 S. Zampolli, I. Elmi, J. Sturmann, S. Nicoletti, L. Dori, G. C. Cardinali, *Sens. Actuators, B* **2005**, *105*, 400.
26 L. F. Nazar, Z. Zhang, D. Zinkweg, *J. Am. Chem. Soc.* **1992**, *114*, 6239.
27 N. Sukpirom, C. O. Oriakhi, M. M. Lerner, *Mater. Res. Bull.* **2000**, *35*, 325.
28 L. F. Nazar, Z. Zhang, D. Zinkweg, *J. Am. Chem. Soc.* **1992**, *114*, 6239.
29 G. R. Goward, T. A. Kerr, W. P. Power, L. F. Nazar, *Adv. Mater.* **1998**, *10*, 449.
30 N. Sukpirom, C. O. Oriakhi, M. M. Lerner, *Mater. Res. Bull.* **2000**, *35*, 325.
31 P. J. Hagrman, R. L. LaDuca, Jr., H.-J. Koo, R. R. Rarig, Jr., R. C. Haushalter, M.-H. Whangbo, J. Zubieta, *Inorg. Chem.* **2000**, *39*, 4311.
32 S. Ke, M. Ying, C. Ya-an, C. Zhao-hui, J. Xue-hai, Y. Jian-nian, *Chem. Mater.* **2001**, *13*, 250.
33 I. P. Silva Filho, J. C. O. Santos, M. M. Conceição, L. M. Nunes, I. M. G. Santos, A. G. Souza, *Mater. Lett.* **2005**, *59*, 2510.
34 R. F. de Farias, *Mater. Chem. Phys.* **2005**, *90*, 302.
35 D. M. Thomas, E. M. McCarron, III, *Mater. Res. Bull.* **1986**, *21*, 945.
36 T. Ivanova, A. Szekeres, M. Gartner, D. Gogova, K. Gesheva, *Electrochim. Acta* **2001**, *46*, 2215.
37 T. Ivanova, A. Szekeres, K. Gesheva, *Mater. Lett.* **2002**, *53*, 250.
38 T. Itoh, I. Matsubara, W. Shin, N. Izu, *Thin Solid Films* **2006**, *515*, 2709.
39 J. Wang, I. Matsubara, W. Shin, N. Izu, N. Murayama, *Thin Solid Films* **2006**, *514*, 329.
40 J. Brandrup, E. H. Immergut, *Polymer Handbook*, 3rd ed., John Wiley & Sons, **1989**, pp. 519–559.
41 P. A. Small, *J. Appl. Chem.* **1953**, *3*, 71.
42 K. L. Hoy, *J. Paint Technol.* **1970**, *42*, 76.